

Separation Criterion for Turbulent Boundary Layers Via Similarity Analysis

Luciano Castillo

Xia Wang

Rensselaer Polytechnic Institute,
Department of Mechanical, Aerospace and
Nuclear Engineering,
Troy, NY 12180

William K. George

Chalmers University of Technology,
Department of Thermo and Fluid Dynamics,
SE-412 96 Göteborg,
Sweden

By using the RANS boundary layer equations, it will be shown that the outer part of an adverse pressure gradient turbulent boundary layer tends to remain in equilibrium similarity, even near and past separation. Such boundary layers are characterized by a single and constant pressure gradient parameter, Λ , and its value appears to be the same for all adverse pressure gradient flows, including those with eventual separation. Also it appears from the experimental data that the pressure gradient parameter, Λ_θ , is also approximately constant and given by $\Lambda_\theta = 0.21 \pm 0.01$. Using this and the integral momentum boundary layer equation, it is possible to show that the shape factor at separation also has to within the experimental uncertainty a single value: $H_{sep} \cong 2.76 \pm 0.23$. Furthermore, the conditions for equilibrium similarity and the value of H_{sep} are shown to be in reasonable agreement with a variety of experimental estimates, as well as the predictions from some other investigators. [DOI: 10.1115/1.1758262]

1 Introduction

Turbulent boundary layer separation is a very important area of research, particularly in the design of airfoils, diffusers and so on. The strongest possible adverse pressure gradient is maintained so that airfoils can achieve maximum lift or a diffusers can obtain maximum pressure recovery. If separation occurs, however, it causes many new complications. For example, separation reduces the lift of an airfoil, and it will also increase the required size of a diffuser. Separation in a turbulent boundary layer is very complex, and it happens as a process instead of a single event as in the laminar case, Simpson et al. [1,2] and Kline et al. [3] etc. In the 1980s the extensive work of Simpson [2,4] led to new insight and definitions for separation in the turbulent boundary layer. Some of the most relevant definitions are:

- Incipient Detachment (ID): the reverse flow occurs occasionally about 1% of the time.
- Intermittent Transitory Detachment (ITD): the reverse flow occurs about 20% of the time.
- Transitory Detachment (TD): the instantaneous back flow occurs 50% of the time.
- Detachment (D): it occurs when the time averaged wall shear stress is zero.

Recent experimental data [2,5,6] suggests that the location where the instantaneous back flow coefficient is about 50% corresponds to the position where the average skin friction is zero.

Many researchers have tried to investigate this process, to characterize separation, and to predict the detachment position. The classic log-law for the velocity profile does not work for the separation flow since the velocity scaling, u_τ , is zero at the separation position. Driver [7] and Schofield [8]. In the 1950s, Stratford [9] introduced an empirical criterion based on the pressure coefficient to predict the point of separation. He further argued that the inner (or near wall) velocity profiles should be scaled using:

$$U_{sep} = \frac{\nu}{\rho} \frac{dP_\infty}{dx} \quad (1)$$

and the inner length scaled using

Contributed by the Fluids Engineering Division for publication in the JOURNAL OF FLUIDS ENGINEERING. Manuscript received by the Fluids Engineering Division October 4, 2001; revised manuscript received November 8, 2003. Associate Editor: T. B. Gatski.

$$\eta_{sep} = \frac{1}{\rho\nu} \frac{dP_\infty}{dx} \quad (2)$$

instead of the usual Prandtl variables, u_* and ν/u_* . These scalings are known as the "Stratford variables," and clearly are necessary because of the vanishing of the shear stress at separation (cf., Tennekes and Lumley 1972 [10] or from more recent perspectives, George and Castillo 1993 [11], Skote and Henningson [12].) These near wall results are not of interest in this paper which focuses on the outer boundary layer and its implications for separation.

In the 1960s and 1970s Kline and his co-investigators established correlation parameters for separation in terms of the shape factor, H , and the ratio of displacement thickness to the boundary layer thickness, δ_*/δ . In particular, Sandborn and Kline [13] suggested that the shape factor at separation was given by,

$$H = 1 + \frac{1}{1 - \delta_*/\delta}, \quad (3)$$

where δ_*/δ must be determined at the point of separation. They further showed that the shape factor is 2.7 at the Intermittent Transitory Detachment (ITD) position. In subsequent work, Kline, Bardina and Strawn [3] developed a one parameter model and concluded that the shape factor was given by $H = 2.7$ at the ITD position and $H = 4.0$ at the separation position.

There are a number of other empirical separation criteria which have been proposed. Sajben and Liao [14] assumed that detachment occurs where the normalized specific momentum defect reaches a maximum as a function of the shape factor; they found a value of the shape factor of 2.7 for ITD turbulent boundary layer. Cebeci and Bradshaw [15] have reported that separation takes place when the values of H fall in the range of $1.8 \leq H_{sep} \leq 2.4$. By contrast, Senoo and Nishi [16] proposed that:

$$H_{sep} = 1.8 + 7.5 \left. \frac{\delta_*}{W} \right|_{sep} \quad (4)$$

for flow in diffusers, where W is the passage width at the point of separation, and δ_* is determined at the point of separation as well. A similar empirical form, which shows a linear relationship between H and χ_w , can be found in the experiment carried out by Dengel and Fernholz [5] (and more recently by Gustavsson [17]) as:

$$H \approx 2.2 + 1.4\chi_w, \quad (5)$$

where χ_w is the back flow coefficient and its value is between 0.20 and 0.70 for this experiment. Meanwhile, Dengel and Fernholz [5] showed that the shape factor H is $2.85 \pm 0.1\%$ at $\chi_w = 50\%$ where the boundary layer is presumed to separate when $\bar{\tau}_w = 0$ (detachment).

Schofield [8] proposed a separation criterion based on the Schofield-Perry analysis [18], and found a shape factor of 3.3 at the separation position. His results, however, were partially based on the measurements by Simpson and his collaborators [1,2] which misidentified the location of transitory detachment, at least according to Dengel and Fernholz [5]. Alving and Fernholz [6] made similar measurements as Dengel and Fernholz [5] for the asymmetric boundary layer with separation. Their results are consistent with each other, yielding shape factors of 2.85 ± 0.1 and 2.76 for Dengel and Fernholz [5] and Alving and Fernholz [6], respectively.

The entire question of where separation occurs experimentally is considerably complicated by the fact that the skin friction is very hard to determine within the boundary layer, and even worse when the shear stress is near zero. The hot-wire anemometer has been the classical tool to measure the velocity profile, but its directional insensitivity limits its application in separating flows for it cannot measure the back-flow velocity accurately. In the past two decades, the advent of new and more precise measuring techniques allowed many investigators to obtain a new understanding of the problem in a physical way. Simpson [1,2] used the directionally sensitive laser anemometer to measure the instantaneous flow direction near the separation region. Dengel and Fernholz [5] and Alving and Fernholz [6] presented pulsed-wire measurements for the separated region and downstream of reattachment region. The PIV has also begun to be applied to separation studies (e.g., Angele and Muhamad-Klingman [19]). Even so, there are still many questions (especially theoretical) that remain to be answered.

The primary goal of this paper is to describe how some recent theoretical advancements in the understanding of turbulent boundary layers lead to a simple separation criterion which is in reasonable agreement with measurements, as well as the results from some other investigators. The detached separation of the steady flow is the main focus in this investigation (cf. Simpson's definitions [2,4,20]). Attention will be given to only the 2-D steady turbulent boundary layer in which the flow is not affected by the turbulence intensity of the free stream. Surface curvature or roughness are also presumed not present in the problem. In brief, the separation is presumed to be caused by the strong adverse pressure gradient alone.

The equilibrium similarity analysis of Castillo and George [21] for the pressure gradient boundary layers will be applied to the *outer* part of adverse pressure gradient boundary layers upstream of and up to separation. These results will then be combined with the integral momentum boundary layer equation to obtain a separation criterion. This separation criterion surprisingly appears to be both quite simple and universal.

2 Review of the Castillo/George Analysis

Castillo and George [21] have set forth in detail the case for considering the outer part of most turbulent boundary layers to be *equilibrium similarity* boundary layers.¹ Surprisingly, the experimental data suggest that only three values of the pressure gradient similarity parameter, Λ (defined below), appear to describe all of the flows considered—one each for zero pressure gradient (ZPG),

¹The term 'equilibrium similarity' should not be confused with the 'equilibrium' boundary layer of Clauser. The Clauser analysis has much more restrictive criteria and is based on approximate equations truncated at first order in u_r/U_∞ , whereas the Castillo/George analysis is valid to third order.

adverse pressure gradient (APG) and favorable pressure gradient (FPG). In this paper only the adverse pressure gradient results will be considered.

For a 2-D, incompressible boundary layer that is statistically steady in the mean the boundary layer equation for the *outer* flow (valid for $y/\delta > 0.1$ typically) reduces to:

$$U \frac{\partial U}{\partial x} + V \frac{\partial U}{\partial y} = -\frac{1}{\rho} \frac{dP_\infty}{dx} + \frac{\partial}{\partial y} [-\langle uv \rangle] + \frac{\partial}{\partial x} [\langle v^2 \rangle - \langle u^2 \rangle], \quad (6)$$

where $U \rightarrow U_\infty$, $\langle uv \rangle \rightarrow 0$ as $y \rightarrow \infty$, $\langle u^2 \rangle$ and $\langle v^2 \rangle \rightarrow 0$ as $y \rightarrow \infty$ as well. This equation, together with the continuity equation, describes the flow exactly in the limit of infinite Reynolds number as long as $y > 100\nu/u_*$ or $y^+ > 100$ typically. It is important to note that after flow separates, the boundary layer thickness may grow drastically, and the boundary layer simplifications are not accurate any longer. Note that the normal stresses components $\langle u^2 \rangle, \langle v^2 \rangle$ have been retained because in APG flows, particularly those approaching separation, their contributions are about 30% (Simpson et al. [4], Dengel and Fernholz [5], Alving and Fernholz [6], Elsberry et al. [22]). The component Reynolds stress equations must also be included in the analysis, but have not been written here since they are the same as for the zero-pressure gradient boundary layer and have been considered in detail elsewhere (cf. George and Castillo 1997 [23]).

The outer scales of the turbulent boundary layer equations must be determined from an equilibrium similarity analysis of the governing equations and boundary conditions, and can not be chosen a priori. George and Castillo [23] applied this concept to the outer boundary layer equations for the ZPG flow, and determined that the mean velocity and Reynolds shear stress scale with U_∞ and $U_\infty^2 d\delta/dx$, respectively. Unlike the Reynolds shear stresses, the Reynolds normal stresses scale with U_∞^2 . Castillo and George [21] extended this similarity analysis to include pressure gradient boundary layers. Their approach and results can be summarized as follows:

Similarity Solution Profiles. The basic assumption is that it is possible to express any dependent variable, in this case the outer deficit velocity, $U - U_\infty$, the outer Reynolds shear stress, $\langle uv \rangle$, and the outer Reynolds normal stresses, $\langle u^2 \rangle, \langle v^2 \rangle$ as a product of two functions; i.e.,

$$U - U_\infty = U_{so}(x) f_{op}(\bar{y}, \delta^+; \Lambda; *); \quad (7)$$

$$-\langle uv \rangle = R_{so}(x) r_{op}(\bar{y}, \delta^+; \Lambda; *); \quad (8)$$

$$\langle v^2 \rangle - \langle u^2 \rangle = R_{no}(x) r_{opn}(\bar{y}, \delta^+; \Lambda; *); \quad (9)$$

where U_{so} , R_{so} , R_{no} are the outer velocity scale, the outer Reynolds shear stress scale, and the Reynolds normal stress difference, all of which depend only on x . Note that all of these *must* be determined from the boundary layer and Reynolds stress equations together with the appropriate boundary conditions. The arguments inside the similarity functions (f_{op} , r_{op} , and r_{opn}) represent the outer similarity coordinate, $\bar{y} = y/\delta_{99}$, the local Reynolds number dependence, $\delta^+ = \delta u_*/\nu$, the pressure gradient parameter, Λ , and any possible dependence on the upstream conditions, $*$, respectively.

Asymptotic Invariance Principle: AIP. This principle can be simply stated as follows: since in the limit as the $Re \rightarrow \infty$ the outer boundary layer equations become independent of the local Reynolds number, therefore any solution to them must also become asymptotically independent of δ^+ . Thus, in this limit, Eq. (7)–Eq. (9) must become independent of local Reynolds number; i.e.,

$$f_{op}(\bar{y}, \delta^+; \Lambda; *) \rightarrow f_{op\infty}(\bar{y}, \Lambda, *); \quad (10)$$

$$r_{op}(\bar{y}, \delta^+; \Lambda; *) \rightarrow r_{op\infty}(\bar{y}, \Lambda, *); \quad (11)$$

$$r_{opn}(\bar{y}, \delta^+; \Lambda; *) \rightarrow r_{opn\infty}(\bar{y}, \Lambda, *); \quad (12)$$

as $\delta^+ \rightarrow \infty$. The subscript ∞ is used to distinguish these infinite Reynolds number solutions from the finite Reynolds number profiles used in Eq. (7)–Eq. (9).

The Transformed Equations. Substituting Eq. (10)–Eq. (12) into Eq. (6) and clearing terms yields:

$$\begin{aligned} & \left[\frac{\delta}{U_{so}} \frac{dU_{\infty}}{dx} + \left(\frac{U_{\infty}}{U_{so}} \right) \frac{\delta}{U_{so}} \frac{dU_{so}}{dx} \right] f_{op\infty} + \left[\frac{\delta}{U_{so}} \frac{dU_{so}}{dx} \right] f_{op\infty}^2 - \left[\frac{U_{\infty}}{U_{so}} \frac{d\delta}{dx} \right. \\ & \quad \left. + \frac{\delta}{U_{so}} \frac{dU_{\infty}}{dx} \right] \bar{y} f'_{op\infty} - \left[\frac{d\delta}{dx} + \frac{\delta}{U_{so}} \frac{dU_{so}}{dx} \right] f'_{op\infty} \int_0^{\bar{y}} f_{op\infty}(\bar{y}) d\bar{y} \\ & = \left[\frac{R_{so}}{U_{so}^2} \right] r'_{op\infty} + \left[\frac{\delta}{U_{so}^2} \frac{dR_{no}}{dx} \right] r_{opn\infty} - \left[\frac{R_{no}}{U_{so}^2} \frac{d\delta}{dx} \right] \bar{y} r'_{opn\infty} \end{aligned} \quad (13)$$

where the term involving $-dP_{\infty}/dx$ has been cancelled by the $\rho U_{\infty} dU_{\infty}/dx$ term from Euler's equation for the external flow.

The Equilibrium Similarity Conditions. For the particular type of “equilibrium” similarity solutions suggested in George [24], all the terms in the governing equations must maintain the same relative balance as the flow develops. These *equilibrium similarity* solutions exist only if all the square bracketed terms have the same x -dependence and are independent of the similarity coordinate, \bar{y} . Thus, the bracketed terms must remain proportional to each other as the flow develops; i.e.,

$$\begin{aligned} \frac{\delta}{U_{so}} \frac{dU_{so}}{dx} & \sim \frac{\delta}{U_{so}} \frac{dU_{\infty}}{dx} \sim \left(\frac{U_{\infty}}{U_{so}} \right) \frac{\delta}{U_{so}} \frac{dU_{so}}{dx} \sim \frac{d\delta}{dx} \sim \left(\frac{U_{\infty}}{U_{so}} \right) \frac{d\delta}{dx} \\ & \sim \frac{R_{so}}{U_{so}^2} \sim \frac{R_{no}}{U_{so}^2} \frac{d\delta}{dx} \sim \frac{\delta}{U_{so}^2} \frac{dR_{no}}{dx} \end{aligned} \quad (14)$$

where ‘ \sim ’ means ‘has the same x -dependence as’.

It is clear that (just as for the zero pressure gradient boundary layer), full similarity (of the “equilibrium-type”) is possible only if

$$U_{so} \sim U_{\infty}, \quad (15)$$

$$R_{so} \sim U_{so}^2 \frac{d\delta}{dx} \sim U_{\infty}^2 \frac{d\delta}{dx} \quad (16)$$

and

$$R_{no} \sim U_{\infty}^2. \quad (17)$$

Note that both the Reynolds shear and normal stress scalings can be shown to be consistent with the Reynolds stress equations themselves (cf. George and Castillo [23]).

Thus, the outer equations do admit to full similarity solutions in the limit of infinite Reynolds number, and these solutions determine the outer scales. No other choice of scales can produce profiles (of the assumed form) which are asymptotically independent of the local Reynolds number, at least unless they reduce to these scales in the limit.

The Pressure Gradient Parameter for Equilibrium Flows. Besides the similarity conditions for the mean velocity and Reynolds stresses, there exist other constraints. In particular,

$$\frac{d\delta}{dx} \sim \frac{\delta}{U_{\infty}} \frac{dU_{\infty}}{dx} \sim \frac{\delta}{\rho U_{\infty}^2} \frac{dP_{\infty}}{dx}. \quad (18)$$

It follows from Eq. (18) that $\Lambda = \text{const}$ is a necessary condition for equilibrium similarity to exist, where the pressure gradient parameter Λ is defined as:

$$\Lambda \equiv \frac{\delta}{\rho U_{\infty}^2} \frac{dP_{\infty}}{dx} = \text{constant}, \quad (19)$$

or equivalently,

$$\Lambda \equiv - \frac{\delta}{U_{\infty}} \frac{dU_{\infty}}{dx} = \text{constant}. \quad (20)$$

A consequence of this is that for $\Lambda \neq 0$, the imposed pressure gradient, dP_{∞}/dx , controls the growth rate of an equilibrium similarity boundary layer. Eq. 20 can be integrated directly to obtain:

$$\delta \sim U_{\infty}^{-1/\Lambda}, \quad (21)$$

so there must be a power law relation between the free stream velocity and the boundary layer thickness. Therefore, an equilibrium similarity boundary layer exists only if the experimental data in log-log plot show a linear relation between the boundary layer thickness (e.g., $\delta_{0.99}$ or $\delta_{0.95}$) and the free-stream velocity (U_{∞} or more typically U_{edge}). There are virtually no measurements for which this is not easily tested [25].

From the perspective of the Castillo/George analysis outlined above, an “equilibrium” boundary layer is one where $\Lambda = \text{constant}$ and $\delta \sim U_{\infty}^{-1/\Lambda}$. Since it is the free stream velocity, U_{∞} (or dP_{∞}/dx), which is usually imposed on the boundary layer by external means, this is a restrictive constraint on δ . As a consequence it provides a powerful experimental test of the theory, and is most easily demonstrated by the linear relationship between $\log(U_{\infty})$ and $\log(\delta)$. Figure 1, taken from Castillo and George [21], shows examples for both favorable (FPG) and adverse (APG) pressure gradient boundary layers. All of the existing experimental data show similar behavior. Thus, by the Castillo/George criterion, it appears that most pressure gradient boundary layer are in equilibrium. In the following section the same test will be applied to equilibrium layers with eventual separation and reattachment.

3 Boundary Layers With Eventual Separation

Figure 2 shows the equilibrium condition of $\log(U_{\infty})$ versus $\log(\theta, \delta_*, \delta)$ for the experimental measurements of Schubauer and Klebanoff [26], Newman [27], Ludweig and Tillmann [28], Simpson et al. [1,2], Alving and Fernholz [6], all of which were made in boundary layers which separated. The linear fit for these measurements continues to and sometimes even after the separation point. Note the close correspondence between the slopes of the plots using δ and θ , and a correspondence that does not hold for δ_* for these separating flows.

Unfortunately there is no explicit relation between θ and δ , although an implicit one can be derived using the momentum integral equation and additional assumptions about the velocity profiles (cf. George and Castillo [23]). For all the adverse pressure gradient boundary layers considered (and as will be shown later), $\Lambda \approx \Lambda_{\theta}$, to within the experimental error, where

$$\Lambda_{\theta} \equiv \frac{\theta}{\rho U_{\infty}^2} \frac{dP_{\infty}}{d\theta/dx} = - \frac{\theta}{U_{\infty}} \frac{dU_{\infty}}{d\theta/dx}, \quad (22)$$

and the θ is the momentum thickness. Most importantly, for all the boundary layers considered, Λ_{θ} also appears to be a single constant. Thus, at least for these boundary layers, the additional semi-empirical relation,

$$\theta \sim U_{\infty}^{-1/\Lambda_{\theta}}, \quad (23)$$

is at least approximately valid. Clearly this is satisfied for the APG data of Fig. 2.

Table 1 lists all the linear fit results of Fig. 2. It is clear that there is a good linear relationship between the $\log(U_{\infty})$ and both $\log(\theta)$ and $\log(\delta)$, exactly like the APG boundary layers which did not separate. Thus, even though the boundary layer approaches separation, the outer flow apparently tends to remain in equilibrium similarity, and its state can be characterized by either Λ or Λ_{θ} , at least until the boundary layer equations themselves break down. This is important, since the *theory* depends only on δ , and θ can only be inferred from the momentum integral (cf. George and Castillo [23]). Note that the average value $\Lambda = 0.23$ is slightly

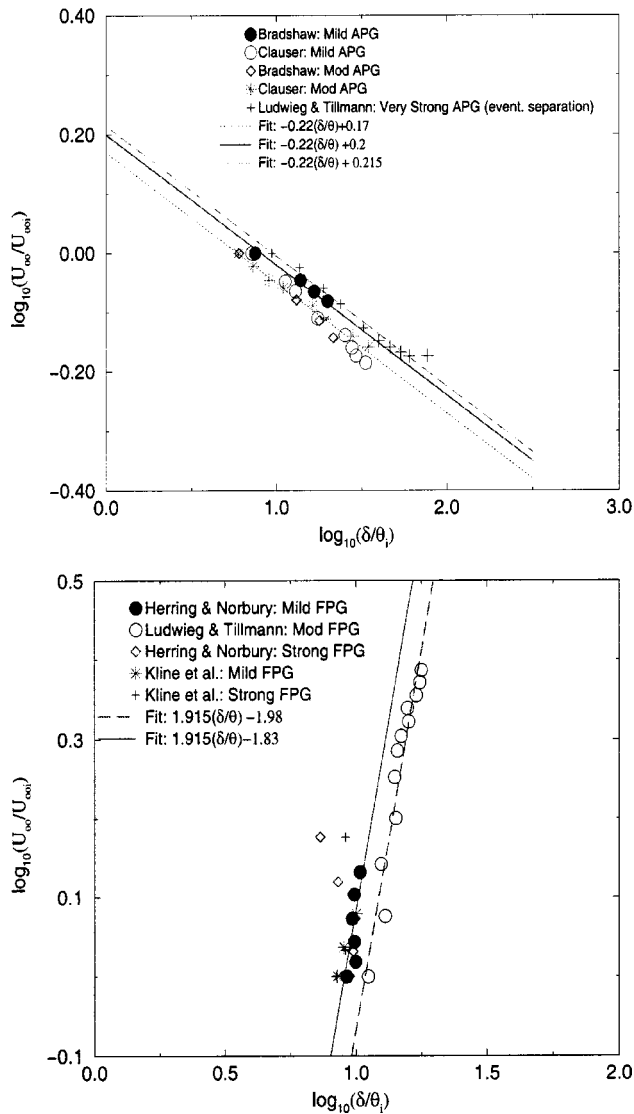


Fig. 1 Top: Plots of U_∞ versus δ_{99} for APG data. **Bottom:** Plots of U_∞ versus δ_{99} for FPG data. Both plots are normalized with U_{x_i} and θ_i for first measured location. The data have been normalized by the free stream velocity and the momentum thickness at the most upstream position.

higher than the value of 0.22 for equilibrium adverse pressure gradient boundary layer suggested by Castillo and George [21], and slightly higher than the average of the Λ_θ values.

Figure 3, shows the same experimental data of Fig. 2. but now characterized with the single average value of $\Lambda_\theta=0.21$. Clearly, all the measurements with eventual separation can also be characterized by a single value. If the constancy of this value was not a surprise before, its applicability to these boundary layers certainly is.

4 The Integral Momentum Equation and the Separation Criterion

The integral boundary layer equation can be written as

$$\frac{C_f}{2} = \frac{d\theta}{dx} - (2+H) \frac{\theta}{\rho U_\infty^2} \frac{dP_\infty}{dx} \quad (24)$$

This can be rewritten using the definition for the pressure parameter Λ_θ as:

$$\frac{C_f}{2} = \frac{d\theta}{dx} [1 - (2+H)\Lambda_\theta] \quad (25)$$

Using the definition for separation by Simpson [2], the mean shear stress $C_f=0$ but $d\theta/dx \neq 0$ at the same point. Then the above integral boundary layer equation at separation reduces to,

$$H_{sep} = \frac{1}{\Lambda_\theta} - 2 \quad (26)$$

This form of the integral equation would be of little use if it was not for the fact that the log-log plots show that the equilibrium similarity theory appears to describe the outer boundary layer almost and perhaps beyond separation with a constant value, $\Lambda_\theta \cong 0.21 \pm 0.01$. It follows immediately that the value of the shape factor at separation is given by $H_{sep} \cong 2.76 \pm 0.23$. This is an amazingly simple result, and is determined entirely by the equilibrium similarity of the outer boundary layer, with no assumptions at all about the inner part.

Table 2 shows the shape factor at separation from various experiments cited previously, along with the present similarity analysis results for shape factor. The experimental values are those provided by the original authors even though the methods of determination varied. Notice that the experimental data studied here include the classical experimental data of Schubauer and Klebanoff [26], Newman [27], and Ludwig and Tillmann [28], in which they use hot-wire as a measurement tool. Because of directional insensitivity of hot-wire, they could not give an exact description of separation location in the flow. Therefore, only the last measured position is shown here, which could be regarded as the intermittent separation point. Simpson [2,1] used an LDA measured the velocity profile in the separation region, and the intermittent detachment region was interpolated from the experimental data. Alving and Fernholz [6] used an asymmetric boundary layer flow with eventual separation and reattachment region, and a pulse-wire to measure the back flow.

Comparing the experimental result with the current result, the new result is remarkably successful, especially given the uncertainty of the data, both for Λ_θ and the value of H at separation. In addition, notice that we are seeking the shape factor at the separation position. However, this result seems to describe the ITD position for the some of classical experiments. For the relatively new experiments, this value proves very successful.

It should be noted that the value of $\Lambda_\theta=0.21$ is a composite value obtained by regression fits to many data sets as shown in Table 2 and Fig. 3. The success of this value is illustrated by figures in this paper. The individual estimates, however, varied by as much as ± 0.01 from the composite value. Thus, the individual estimates of H_{sep} could also vary as $2.5 < H_{sep} < 3.0$. This is a large range indeed, and certainly spans the range of the experimental values in the table. Clearly, there is a demand for new experiments to determine whether the values of Λ_θ and H_{sep} are universal, or whether the differences are real.

The proposed theoretical value is very close to some of the previous empirical results discussed earlier.

- First, the proposed shape factor is consistent with the result by Sandborn and Kline [13], Eq. 3, which shows that the incipient separation occurs when $\delta^*/\delta_{sep}=0.43$ and $H_{sep}=2.7$. Working backwards, the uncertainty range of H from the present theory using the data cited above suggests that δ^*/δ at separation should be in the range of $0.33 \leq \delta^*/\delta \leq 0.5$. The relation between the present theory and the Sandborn/Kline correlation can best seen by plotting H versus δ^*/δ as shown in Fig. 4. The vertical lines show the range of the Sandborn/Kline values, the horizontal lines the uncertainty range of H from the present theory. The top plot in Fig. 4. shows all the equilibrium turbulent boundary layers with very strong adverse pressure gradient, [26,29,30,31,32], but without separation. It is obvious that all of these measurements are below the separation zone. The bottom plot in Fig. 4. shows all the

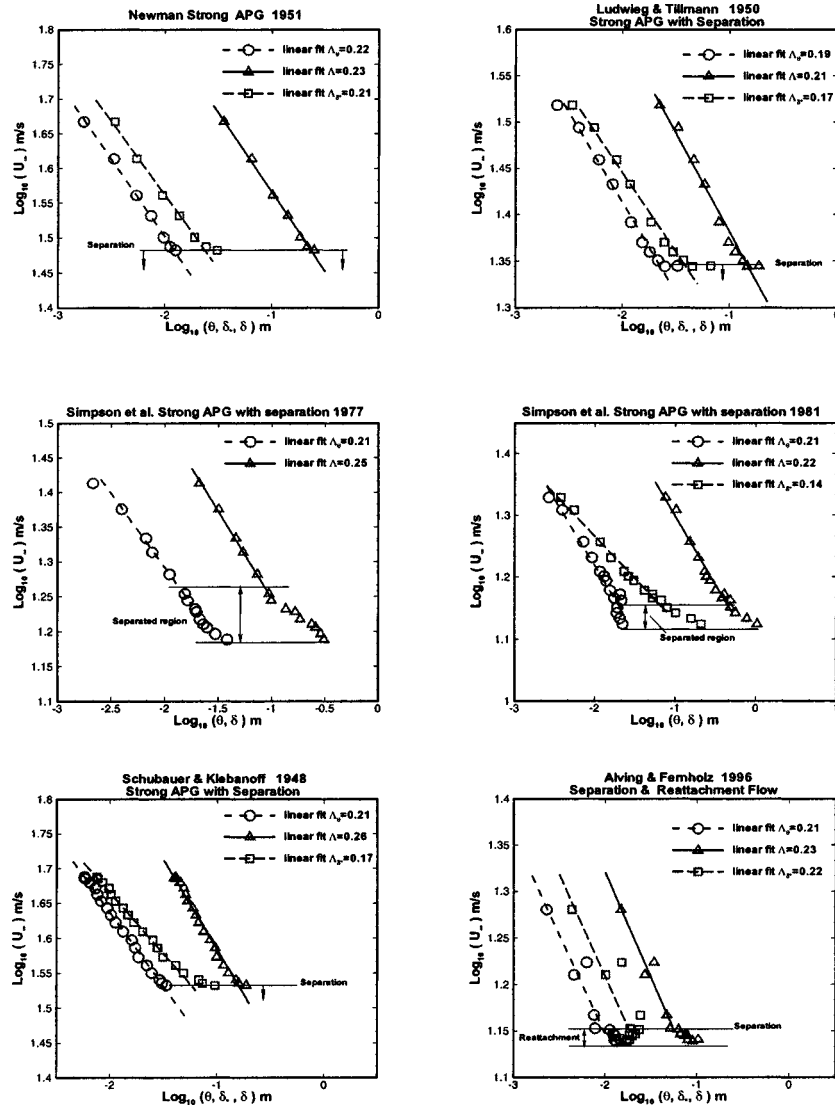


Fig. 2 Equilibrium boundary layers with eventual separation: log-log plots of U_∞ versus θ , δ_* and δ .

experiments with separation. The separated or intermittent separation positions have been circled. It is clear that most of these points fall into the separation region, which is remarkable considering the difficulty of the actual measurement. Therefore, Fig. 4 provides a useful picture to describe the separation zone, and emphasizes that separation in the turbulent boundary layer is perhaps a process instead of a single event (as indicated by Simpson [2]).

- Second, this result agrees with Kline et al. [3] one-parameter correlation prediction. The shape factor at the intermittent detach-

ment is shown to be 2.7. Notice that the intermittent detachment here refers to $\gamma_w = 5\% - 20\%$ instead of $\gamma_w = 20\%$ by Simpson et al. [2].

- Third, this investigations is also in agreement with the recent study by Sajben and Liao [14]. They assumed that the normalized specific momentum defect reaches a maximum value at detachment position, which experimentally corresponds to ITD with $H = 2.7$.

- Forth, this result is consistent with the latest experimental data for separation by Alving and Fernholz [6]. Using a pulse-wire as the measurement tool, a shape factor of 2.78 is found at the separation position. Also this result is within the range of 2.85 ± 0.1 reported by the Dengel and Fernholz [5].

Finally, in addition to the experimental evidence cited above, there are a number of indirect inferences which can be made from industrial practice and from laboratory experiments in which the boundary layers did not separate. For example, one common design criterion for industrial turbine designers to avoid separation on compressor blades is to *not* allow the shape factor to exceed 2.5 (Hall [29]). Another example is the recent experiment of Els-

Table 1 The pressure parameter for turbulent boundary layers with separation

Experiments (separation)	Λ_θ	Λ	Λ_{δ^+}
Newman [27]	0.223	0.228	0.212
Ludweig & Tillmann [28]	0.194	0.213*	0.171
Alving & Fernholz [6]	0.212	0.226	0.219
Simpson et al. [2]	0.214	0.222	0.137
Simpson et al. [1]	0.212	0.251	—
Schubauer & Klebanoff [26]	0.213	0.257*	0.174
R.M.S.	0.21 ± 0.01	0.23 ± 0.02	0.19 ± 0.03

* δ_{95} is used instead of δ_{99}

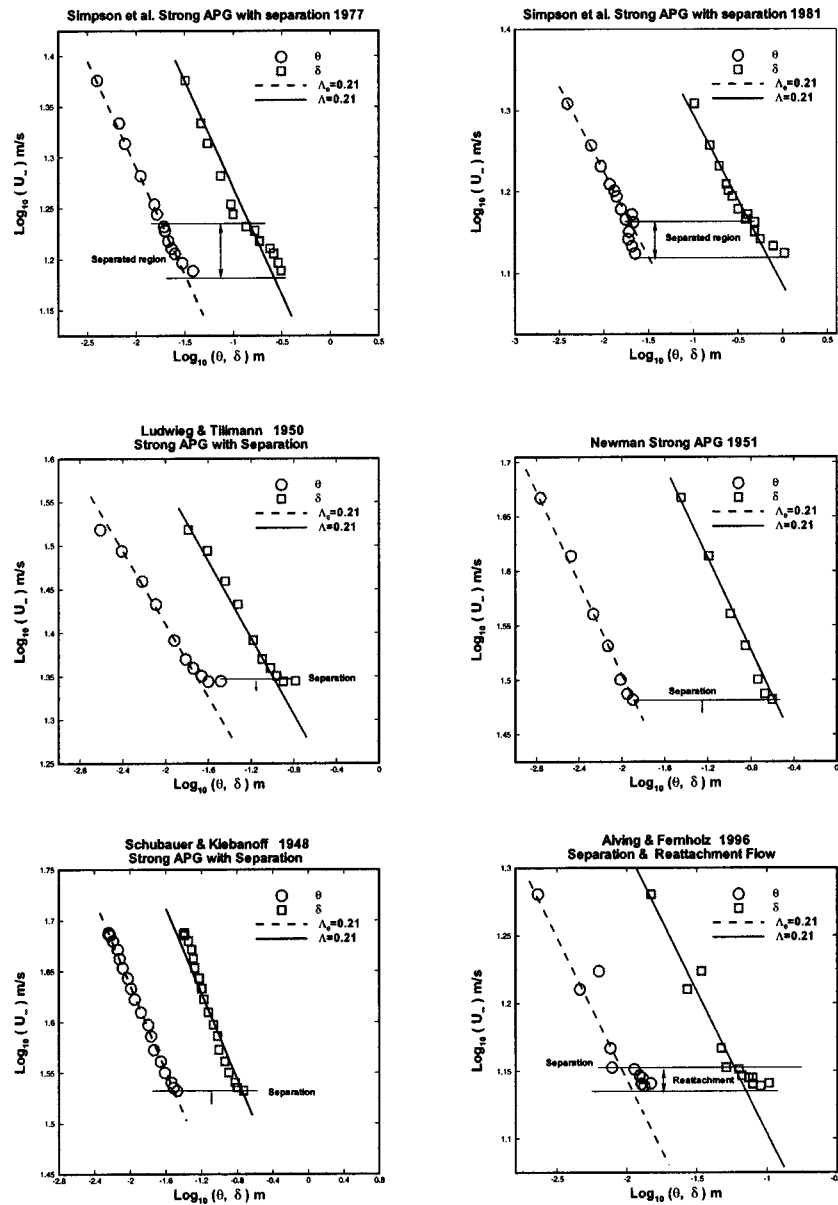


Fig. 3 Equilibrium boundary layers with eventual separation: log-log plots of U_∞ versus δ and θ .

berry et al. [22] that created an equilibrium boundary layer on the verge of separation, but found it necessary to keep the shape factor below 2.6.

5 Summary and Conclusions

Using the RANS equations and similarity analysis, it was shown that:

- The outer part of separating boundary layers are also equilibrium similarity boundary layers characterized by a constant pressure parameters.
- The pressure parameter Λ_θ is nearly same for all the APG flows with eventual separation; in particular, $\Lambda_\theta = 0.21 \pm 0.01$.
- It is possible to characterize boundary layers at separation by $H_{sep} = 2.76 \pm 0.23$. This value of shape factor is in close agree-

Table 2 The values for the shape factor H

Experiment	Λ_θ	H_{sep}	$H = \frac{1}{\Lambda_\theta} - 2$	Position	Boundary layer description
Schubauer & Klebanoff [13]	0.21	2.84	2.76	the last point	airfoil type flow-hot-wire
Newman [27]	0.22	2.46	2.55	the last point	airfoil type flow-hot-wire
Ludwig & Tillmann [28]	0.19	2.04	3.26	the last point	diverging channel flow-hot-wire
Simpson et al. [1]	0.21	2.62	2.76	ITD	airfoil type flow-LDA
Simpson et al. [2]	0.21	2.97	2.76	ITD	airfoil type flow-LDA
Alving & Fernholz [6]	0.21	2.78	2.76	Detachment	asymmetric flow-Pulse-wire

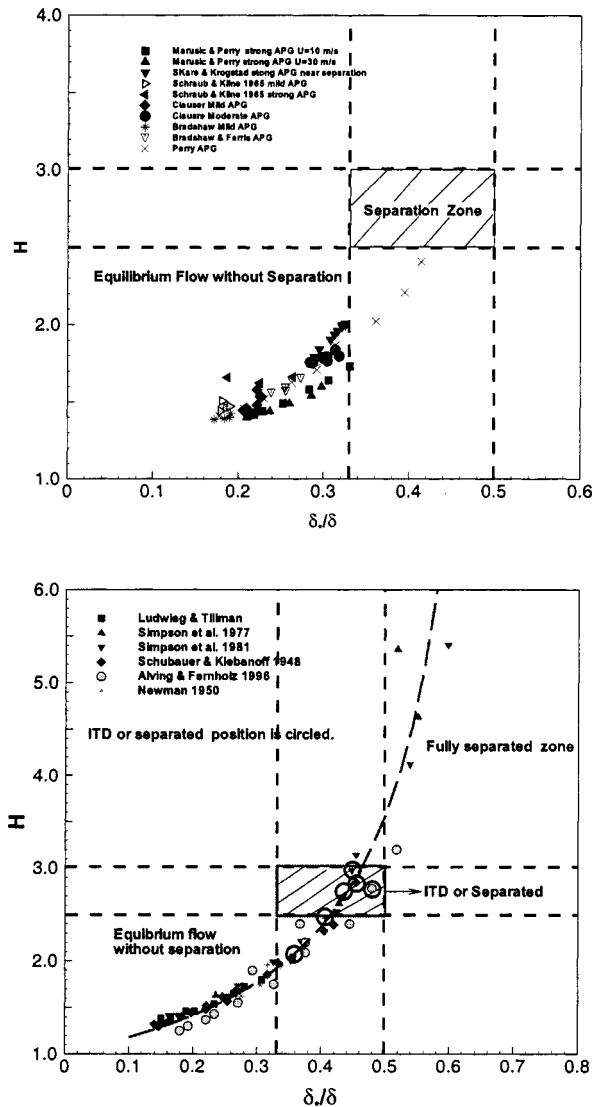


Fig. 4 Top: H and δ_*/δ correlation for equilibrium APG flows. bottom: H and δ_*/δ correlation for strong APG flows with separation.

ment with the ITD position for the experimental data studied here. This result also agrees with other investigations for the ITD position.

In conclusion, it appears that even separating boundary layers have a tendency to remain in an equilibrium similarity state, at least the outer part of the boundary layer. These equilibrium boundary layers are characterized by a constant pressure parameter $\Lambda_\theta = 0.21$. Nonetheless, although a correlation for separation has been established *if it occurs*, the important task of explaining *why* it happens and *how* it can be predicted remains. Perhaps equilibrium similarity considerations will ultimately provide this insight as well.

Acknowledgment

The authors are very thankful to Professor Wygnanski from Arizona State University and Professor Marusic from University of Minnesota for providing their original data, and to the reviewers for their insightful comments.

Nomenclature

- H = shape factor
- H_{sep} = shape factor at separation
- R_{so} = outer Reynolds stress scale
- U_{sep} = velocity at separation
- U_{so} = unknown outer velocity scale
- U_∞ = free stream velocity
- $U_\infty - U$ = velocity deficit
- u_* = friction velocity, $u_*^2 = \tau_w / \rho$
- Λ = pressure parameter, $(\delta / \rho U_\infty^2 d\delta/dx)(dP_\infty/dx)$
- δ = boundary layer thickness, δ_{99}
- θ = momentum thickness, $\int_0^\infty (U/U_\infty)(1 - U/U_\infty)dy$
- Λ_{δ_*} = pressure parameter, $(\delta_* / \rho U_\infty^2 d\delta_*/dx)(dP_\infty/dx)$
- Λ_θ = pressure parameter, $(\theta / \rho U_\infty^2 d\theta/dx)(dP_\infty/dx)$
- δ_* = displacement thickness, $\int_0^\infty (1 - U/U_\infty)dy$
- θ_i = momentum thickness at first measured position
- $*$ = (unknown) dependence on upstream conditions

References

- [1] Simpson, R. L., and Strickland, J. H., 1977, "Features of a separating turbulent boundary layer in the vicinity of separation," *J. Fluid Mech.*, **79**, pp. 553–594.
- [2] Simpson, R. L., and Chew, Y. T., 1981, "The structure of a separating turbulent boundary layer. Part 1. Mean flow and Reynolds stresses," *J. Fluid Mech.*, **113**, pp. 23–51.
- [3] Kline, S. J., Bardina, J. G., and Strawn, R. C., 1983, "Correlation of the detachment of two-dimensional turbulent boundary layers," *AIAA J.*, **21**, pp. 68–73.
- [4] Simpson, R. L., and Chew, Y. T., 1981, "The structure of a separating turbulent boundary layer. Part 2. Higher-order turbulence results," *J. Fluid Mech.*, **113**, pp. 53–73.
- [5] Dengel, P., and Fernholz, H. H., 1990, "An experimental investigation of an incompressible turbulent boundary layer in the vicinity of separation," *J. Fluid Mech.*, **212**, pp. 615–636.
- [6] Alving, A. E., and Fernholz, H. H., 1995, "Turbulence measurements around a mild separation bubble and down-stream of reattachment," *J. Fluid Mech.*, **322**, pp. 279–328.
- [7] Driver, D. M., 1991, "Reynolds Shear stress measurements in a separated boundary layer flow," AIAA-91-1787, 22nd Fluid Dynamics, Plasma Dynamics, and Lasers Conference.
- [8] Schofield, W. H., 1986, "Two-dimensional Separating Turbulent Boundary layers," *AIAA J.*, **24**, No. 10, pp. 1611–1620.
- [9] Stratford, B. S., 1959, "The prediction of separation of the turbulent boundary layer," *J. Fluid Mech.*, **5**, pp. 1–16.
- [10] Tennekes, H., and Lumley, J. L., 1972, *A First Course in Turbulence*, MIT Press, Cambridge, MA.
- [11] George, W. K., and Castillo, L., 1993, "Boundary Layers with Pressure Gradient: Another look at the equilibrium boundary layer," *Near Wall Turbulence* (So, R. et al. eds.), pp. 901–910, Elsevier, NY.
- [12] Skote, M., and Henningson, D. S., 2002, "Direct numerical simulation of a separated turbulent boundary layer," *J. Fluid Mech.*, **471**, pp. 107–136.
- [13] Sandborn, V. A., and Kline, S. J., 1961, "Flow models in boundary-layer stall inception," *J. Basic Eng.*, **83**, pp. 317–327.
- [14] Sajben, M., and Liao, Y., 1995, "Criterion for the detachment of laminar and turbulent boundary layers," *AIAA J.*, **33**, No. 11, pp. 2114–2119.
- [15] Cebeci, T., and Bradshaw, P., 1977, *Momentum Transfer in Boundary Layers*, McGraw Hill Book Co., New York, pp. 194.
- [16] Senoo, Y., and Nishi, M., 1975, "Prediction of flow separation in a diffuser by a boundary layer calculation," *ASME J. Fluids Eng.*, **99**, pp. 379–389.
- [17] Gustavsson, J., 1998, "Experiments on turbulent flow separation," Master's thesis, Royal Institute of Technology, Sweden.
- [18] Perry, A. E., and Schofield, W. H., 1973, "Mean velocity and shear stress distributions in turbulent boundary layers," *Phys. Fluids*, **16**, 12, pp. 2068–2074.
- [19] Angele, K., and Muhammad-Klingman, B. 2003 "Self-similarity velocity scalings," in Ph.D. dissertation of K. Angele, 'Experimental studies of turbulent boundary layer separation and control,' Dept. of Mechanics, KTH, Stockholm, Sweden, 81–105.
- [20] Simpson, R. L., 1989, "Turbulent boundary-layer separation," *Annu. Rev. Fluid Mech.*, **21**, pp. 205–234.
- [21] Castillo, L., and George, W. K., 2001, "Similarity analysis for turbulent boundary layer with pressure gradient: outer flow," *AIAA J.*, **39**, No. 1, pp. 41–47.
- [22] Elsberty, K., Loeffler, J., Zhou, M. D., and Wygnanski, I., 2000, "An experimental study of a boundary layer that is maintained on the verge of separation," *J. Fluid Mech.*, **423**, pp. 227–262.
- [23] George, W. K., and Castillo, L., 1997, "Zero-pressure-gradient turbulent boundary layer," *Appl. Mech. Rev.*, **50**, pp. 689–729.
- [24] George, W. K., 1995, "Some new ideas for similarity of turbulent shear flows," *Turbulence, Heat and Mass Transfer*, ed. by K. Hanjalic and J. C. F. Pereira, Begell House, NY.
- [25] Castillo, L., 1997, "Similarity Analysis of turbulent boundary layers," Ph.D.

Dissertation, Department of Mechanical and Aerospace Engineering, SUNY/ Buffalo, Buffalo, NY.

- [26] Schubauer, G. B., and Klebanoff, P. S., 1951, "Investigation of separation of the turbulent boundary layer," NACA Report 1030, NACA Technical Note 2133.
- [27] Newman, B. G., 1951, "Some Contributions to the Study of the Turbulent Boundary Near Separation," *Austr. Dept. Supply Rep.* ACA-53.
- [28] Ludwig, H., and Tillmann, W., 1950, "Investigations of the wall shearing stress in turbulent boundary layers," NACA TM 1285.
- [29] Håll, U., 2003 private communication to WKG by U. Håll, Professor of Turbomachinery at Chalmers Univ. of Technology, Gothenburg, Sweden.
- [30] Skåre, P. E., and Krogstad, P., 1994, "A turbulent equilibrium boundary layer near separation," *J. Fluid Mech.*, **272**, pp. 319–348.
- [31] Coles, D. E., and Hirst, E. A., 1968, Computational of Turbulent Boundary Layers-1968 AFOSR-IFP-stanford conference, Vol. II.
- [32] Marusic, I., and Perry, A. E., 1995, "A wall-wake model for the turbulence structure of boundary layers. Part 2. Further experimental support," *J. Fluid Mech.*, **298**, pp. 389–407.